International Immunopharmacology 123 (2023) 110711

Contents lists available at ScienceDirect

International Immunopharmacology

journal homepage: www.elsevier.com/locate/intimp

IL-33 promotes sciatic nerve regeneration in mice by modulating macrophage polarization

Shukur Wasman Smail [a,b], Shang Ziyad Abdulqadir [b], Zhikal Omar Khudhur [c,*], Sonia Elia Ishaq [b], Abdullah Faqiyazdin Ahmed [d], Mohammad B. Ghayour [e], Arash Abdolmaleki [f,*]

[a] Department of Medical Microbiology, College of Science, Cihan University-Erbil, Kurdistan Region, Iraq
[b] Department of Biology, College of Science, Salahaddin University-Erbil, Kurdistan Region, Iraq
[c] Department of Biology Education, Faculty of Education, Tishk International University - Erbil, Kurdistan Region, Iraq
[d] KBMS, College of Medicine, Hawler Medical University, Erbil, Kurdistan Region, Iraq
[e] Department of Biology, Faculty of Science, Ferdowsi University of Mashhad, Mashhad, Iran
[f] Department of Biophysics, Faculty of Advanced Technologies, University of Mohaghegh Ardabili, Namin, Iran

ARTICLE INFO

Keywords:
IL-33
Sciatic Nerve
Macrophage
Cytokine
Inflammation

ABSTRACT

Despite the innate regenerative capacity of peripheral nerves, regeneration after a severe injury is insufficient, and sensorimotor recovery is incomplete. As a result, finding alternative methods for improving regeneration and sensorimotor recovery is essential. In this regard, we investigated the effect of IL-33 treatment as a chemokine with neuroprotective properties. IL-33 can facilitate tissue healing by potentiating the type 2 immune response and polarizing macrophages toward the pro-healing M2 phenotype. However, its effects on nerve regeneration remain unclear. Therefore, this research aimed to evaluate the neuroprotective effects of IL-33 on sciatic nerve injury in male C57BL/6 mice. After crushing the left sciatic nerve, the animals were given 10, 25, or 50 μg/kg IL-33 intraperitoneally for seven days. The sensorimotor recovery was then assessed eight weeks after surgery. In addition, immunohistochemistry, ELISA, and real-time PCR were used to assess macrophage polarization, cytokine secretion, and neurotrophic factor expression in the injured nerves. IL-33 at 50 and 25 μg/kg doses could significantly accelerate nerve regeneration and improve sensorimotor recovery when compared to 10 μg/kg IL-33 and control groups. Furthermore, at 50 and 25 μg/kg doses, IL-33 polarized macrophages toward an M2 phenotype and reduced proinflammatory cytokines at the injury site. It also increased the mRNA expression of NGF, VEGF, and BDNF. These findings suggest that a seven-day IL-33 treatment had neuroprotective effects in a mouse sciatic nerve crush model, most likely by inducing macrophage polarization toward M2 and regulating inflammatory microenvironments.

1. Introduction

Following peripheral nerve injury (PNI), neurons and Schwann cells (SCs) transform into regenerative phenotypes. The distal segment of injured nerves also undergoes a multistep repair process, including Wallerian degeneration, axonal regrowth, and target organ reinnervation [1–3]. Among these steps, Wallerian degeneration provides a permissive environment for axonal regeneration and serves as a preface to axonal regeneration [4,5]. However, successful Wallerian degeneration and axon regeneration are dependent on SCs transdifferentiation and immune cell infiltration [6,7]. The immune cells, especially macrophages, play a significant role in Wallerian degeneration through distal axon degeneration, inhibitory debris clearance, neurotrophic factor expression, regulatory cytokine secretion, and extracellular

Abbreviations: PNI, Peripheral nerve injury; ECM, Extracellular matrix; VEGF, Vascular endothelial growth factor; IL-33, Interleukin-33; IL-1RAP, IL-1 receptor accessory protein; MAPK, Mitogen-activated protein kinase; NF-κB, Nuclear factor-κB; SFI, Sciatic functional index; DMSO, Dimethyl sulfoxide; PWRL, Thermal paw withdrawal reflex latency; CMAP, Compound muscle action potential; BDNF, Brain-derived neurotrophic factor; NGF, Nerve growth factor; CNS, Central nervous system; SCI, Spinalcordinjury.

* Corresponding authors at: Department of Biophysics, Faculty of Advanced Technologies, University of Mohaghegh Ardabili, Namin, Iran (Arash Abdolmaleki), Department of Biology Education, Faculty of Education, Tishk International University - Erbil, Kurdistan Region, Iraq (Zhikal Omar Khudhur).
E-mail addresses: zhikal.omer@tiu.edu.iq (Z. Omar Khudhur), Abdolmalekiarash1364@uma.ac.ir (A. Abdolmaleki).

https://doi.org/10.1016/j.intimp.2023.110711
Received 11 June 2023; Received in revised form 11 July 2023; Accepted 24 July 2023
Available online 31 July 2023

matrix (ECM) remodeling [8,9]. Macrophages are phagocytic innate immune cells that reside in or infiltrate the peripheral nerve and orchestrate the regeneration process following nerve injury [8,10]. Debris clearance is a critical step in nerve regeneration because the debris acts as a physical barrier and a source of inhibitory signals for the regenerating axons. Debris phagocytosis is performed mainly by SCs and resident or infiltrating macrophages [11]. Furthermore, following PNI-induced hypoxia, macrophages can produce vascular endothelial growth factor (VEGF) and promote angiogenesis in the distal nerve segment [12].

Macrophages in the peripheral nervous system have two phenotypes: classically activated (M1) and alternatively activated (M2), which influence the outcome of nerve regeneration [11,13]. M1 macrophages release pro-inflammatory cytokines (IL-1β, IL-6, TNF-α, etc.), phagocytose debris, and promote the transdifferentiation of SCs into a regenerative state [14]. M1 macrophages are then transformed into M2 macrophages, which release anti-inflammatory cytokines like IL-10 and support nerve regeneration and angiogenesis [1,15]. Evidence suggests that boosting M1 phenotype polarization toward M2 phenotypes is a crucial stage in the nerve regeneration process [16,17]. In the M2 macrophage subtypes, in addition to their common anti-inflammatory effects, they also have their respective functions. Briefly, M2a, M2b, M2c, and M2d macrophages promote cell proliferation, cell maturation, resolution of inflammation, and angiogenesis, respectively. The M2 macrophage subtypes have great therapeutic potential given their documented anti-inflammatory effects and their respective functions in promoting tissue regeneration in engineered nerve tissue models [16,18].

In this regard, interleukin-33 (IL-33), a member of the IL-1 cytokine family, plays a crucial role in immunity following necrosis, injury, and pathogen or allergen exposure [19]. IL-33 also helps to maintain tissue homeostasis and heal tissue injuries. Extracellular IL-33 works by binding to a heterodimeric membrane receptor consisting of the suppression of tumorigenicity 2 (ST2) and IL-1 receptor accessory protein (IL-1RAP) subunits, which recruited myeloid differentiation primary response protein 88 (MyD88) and eventually activated the mitogen-activated protein kinase (MAPK) and nuclear factor-κB (NF-κB) signaling pathways [20]. IL-33 is commonly expressed by epithelial cells, endothelial cells, fibroblasts, and various immune cells, including macrophages, in both healthy and injured tissues [21]. IL-33 and its receptor are also expressed in neurons and glial cells in the central nervous system (CNS). Furthermore, the IL-33/ST2 signaling pathway triggers a cascade of intracellular events that eventually result in local immune responses [21]. Previous research has shown that exogenous IL-33 promotes microglial recruitment and polarization toward the anti-inflammatory (M2) phenotype [22]. Furthermore, evidence suggests that IL-33 can recruit macrophages in a paracrine manner and polarize the macrophages toward an alternatively activated (M2) phenotype [23]. Nevertheless, despite all of the research on IL-33, its impact on PNI is still unclear. Therefore, the present study was conducted to evaluate the neuroprotective effects of IL-33 on sciatic nerve injury in male C57BL/6 mice.

2. Materials and methods

2.1. Animals and experimental groups

All experimental procedures were conducted in accordance with the European Union Council Directive of November 24, 1986(86/609/EEC), and followed the guidelines developed by the ethical committee at the University of Salahaddin (Iraq) with ethic number: 402,165 for the care and use of laboratory animals. Eighty-four 8 –10-week-old male C57BL/6 mice weighing 25 ± 4 g were used in this experiment. Animals were kept in groups of three in Plexiglas cages under temperatures of 22 ± 2 °C and 12-h light–dark cycles with free access to standard rodent chow and clean water *ad libitum*. Six groups of mice (n = 14) were randomly assigned, including a healthy control group; a control group in which the sciatic nerve was crushed without any treatment; a sham control group in which the sciatic nerve was exposed but not crushed; and three groups in which mice were treated intraperitoneally with 10 μg/kg, 25 μg/kg, and 50 μg/kg of recombinant mouse IL-33 (Sigma-Aldrich, SRP3210), respectively, after the sciatic nerve had been crushed. IL-33 was dissolved in phosphate-buffered saline (PBS) as a vehicle and administered daily for seven days after surgery. The doses of IL-33 used in the present study were chosen based on previous research [24,25]. At the end of the experiment, all animals were euthanized by CO2 inhalation, and their bodies were burned in a furnace.

2.2. Surgical method

We used a nerve crush injury as a simple axonotmesis model to avoid the surgical complications and potential variables associated with a nerve transection model [26]. The same surgeon performed the surgeries under aseptic conditions. The mice were anesthetized with ketamine (60 mg/kg) and xylazine (4 mg/kg) intraperitoneally before being placed in a prone position on a heating pad (37 ± 1 °C). Afterward, we employed serrated right-angle forceps (Mixter forceps, Cole Parmer) with a tip width of 2.5 mm to crush the sciatic nerve at 5 mm distal to the sciatic notch. The nerve was compressed twice, each time for 30 s, in perpendicular directions. The lesion site was then labeled using powdered carbon. Finally, the muscles and skin were sutured, and the animals were allowed to recover from anesthesia. All operated animals received a single dose of buprenorphine (0.05 mg/kg) administered subcutaneously as an analgesic immediately following surgery. In addition, to avoid autotomy, bitter nail polish was applied to the operated limb.

2.3. Sciatic functional index (SFI)

The SFI was assessed before surgery and every two weeks for the next eight weeks to determine motor function recovery. In this regard, the mouse with black ink-painted hind limbs was allowed to leave footprints down the white sheet-covered corridor. A blind operator then measured the distance between the third toe tip and the hind limb pads (paw length, PL), the first and fifth toes (toe spread, TS), and the second and fourth toes (intermediary toe spread, ITS) in the injured (E) and healthy contralateral (N) hind limbs. Three prints from each mouse's injured and contralateral healthy hind limbs were measured and averaged. Afterward, measured parameters were entered into the *Bain et al.* (1989) formula for SFI calculation as follows: SFI = -38.3 [(EPL-NPL)/NPL] + 109.5 [(ETS-NTS)/NTS] + 13.3 [(EIT-NIT)/NIT] – 8.8 [27]. SFI scores vary from 0 (normal function) to −100 (complete loss of hindlimb motor function) [28].

2.4. Hot plate test

The thermal paw withdrawal reflex latency (PWRL) was evaluated preoperatively, 2, 4, 6, and 8 weeks after surgery to determine sensory recovery. Mice were restrained above the waist and placed on a hot plate (55 ± 1 °C; PE34, IITC Life Sciences, USA) with their affected hind paw. PWRL was defined as the time elapsed between the hotplate touch and the withdrawal of the hind paw. All assays were performed three times at two-minute intervals, with averages reported. We set the cut-off time to 10 s to avoid injury to the foot tissue [29].

2.5. Electrophysiological evaluation

The compound muscle action potential (CMAP) and onset latency of CMAPs were assessed in the 4th and 8th weeks postoperatively, as previously described [30]. Briefly, the animal was anesthetized using a cocktail of ketamine (60 mg/kg) and xylazine (4 mg/kg) and placed on the heating pad (37 ± 1 °C) in the prone position. A bipolar hook

electrode was placed 5 mm distal to the sciatic notch on moistened skin and used to stimulate the sciatic nerve. An active recording needle electrode (30 G) and a reference needle electrode (30 G) were also inserted into the gastrocnemius muscle belly and the Achilles tendon, respectively. The sciatic nerve was stimulated with supramaximal square-wave pulses of 0.2 ms duration and 0.5 ms intervals to produce the maximum CMAP response. The CMAP signal was captured at 10 kHz, low-pass filtered at 10 Hz, and high-pass filtered at 1 kHz. The healthy contralateral sciatic nerve was used to measure the normal CMAP [31].

2.6. Histomorphometry analysis

Following electrophysiological assessment, animals were euthanized, and the sciatic nerves were harvested 5 to 10 mm below the crush site. The specimens were fixed in 4% paraformaldehyde (PFA) in PBS overnight at 4 °C. The nerve tissue was then dehydrated in a graded ethanol series before being embedded in paraffin overnight. Finally, the samples were cut into 1 μm-thick transverse sections and stained with 1% toluidine blue for light microscopy analysis (Carl Zeiss, Germany). Histomorphometric analysis was performed on a single sciatic nerve cross-section from each mice (a total of ten samples from each group). Since the nerve histomorphometry parameters differ depending on the nerve level, all sections were obtained approximately 7 mm distal to the nerve lesion site. The sciatic nerve cross-sections were imaged at 400x magnification using a light microscope equipped with an Olympus DP72 camera. Ten overlapping photomicrographs were stitched together to cover the entire nerve cross-section in ImageJ (National Institutes of Health, Maryland). The total fiber number in the nerve was then estimated by manually counting axons in 10% of the nerve cross-section. For this purpose, a sampling frame grid was placed on each nerve cross-section image, and a blind observer counted myelinated axons within each sampling field (selected through systematic random sampling), as well as the upper and left borders. The diameters of the axon and fiber were both measured. From these measurements, the thickness of the myelin and the g-Ratio were calculated using the formulas [(fiber diameter-axon diameter)/2] and axon diameter/fiber diameter. The sciatic nerve of the uninjured contralateral limb was considered a healthy control [32].

2.7. Immunohistochemical staining

Two weeks after surgery, immunohistochemical staining was performed to evaluate the macrophage population in the injured nerves. In brief, cold PBS was used to perfuse four animals from each group, followed by a 4% PFA solution in PBS through intracardial injection. Following that, sciatic nerves 5 to 10 mm distal to the crush site were harvested and post-fixed in PBS with a 4% PFA solution for another 24 h. The fixed nerves were cryo-embedded for 24 h in the Tissue Tek O.C.T. compound before being cryo-sectioned at a thickness of 10 μm. The nerve sections were then treated in a blocking solution of 10% fetal bovine serum (FBS; Gibco) in PBS for one hour at room temperature to inhibit non-specific antibody binding. The sections were then incubated overnight at 4°C with the following primary antibody solutions: rat anti-mouse CD68 monoclonal antibody (1:100, IgG2a, Bio-Rad, MCA1957) to determine the total activated macrophages; rat anti-mouse CCR7 monoclonal antibody (1:100, IgG2a, R&D Systems, MAB3477) to identify the M1 macrophages; and rat anti-mouse CD206 monoclonal antibody (1:100, IgG2a, Bio-Rad, MCA2235) to specify the M2a and M2c macrophages. After rinsing in a PBS-triton 0.5% solution, the nerve sections were incubated in a secondary antibody solution containing triton 0.5% for one hour at room temperature. Alexa Fluor 594 (red) mouse anti-rat IgG2a antibody (1:200, Biolegend, 407509) and Alexa Fluor 488 (green) mouse anti-rat IgG2a antibody (1:200, Biolegend, 407514) were used as secondary antibodies. Finally, the stained nerve sections were rinsed with PBS, dried, and then cover-slipped. Following that, they were examined using a fluorescence microscope (Axioskop 2, Zeiss) [33].

2.8. Enzyme-Linked immunosorbent assay (ELISA)

Two weeks after surgery, pro-inflammatory cytokines (IL-6 and IL-1β) and anti-inflammatory cytokines (IL-4 and IL-10) were measured in the sciatic nerves using the ELISA test. In brief, the sciatic nerve was harvested distally from the crush site and homogenized in a mixture of Tris buffer, protease inhibitors, and phosphatase inhibitors. The homogenized nerve was centrifuged, and cytokine concentrations in the supernatants were determined using the IL-1β Mouse ELISA Kit (Abcam; ab197742), the IL-4 Mouse ELISA Kit (Abcam; ab100710), the IL-6 Mouse ELISA Kit (Abcam; ab285330), and the IL-10 Mouse ELISA Kit (Abcam; ab46103). The cytokine concentrations were calculated by measuring the optical density (OD) at 450 nm and plotting a standard curve using standard solutions. The data is presented in pg (cytokine)/mL (medium)/mg (tissue).

2.9. Real-Time polymerase chain reaction (real time-PCR)

Real-time PCR was used to assess the mRNA expression levels of NGF, VEGF, and BDNF two weeks after surgery. In brief, total RNA was extracted from sciatic nerves using a Total RNA Extraction Kit (Promega, USA) according to the manufacturer's protocol. After quantifying RNA quality and yield using a Thermo Fisher Scientific Nanodrop ND-1000 spectrophotometer, 1 μg of total RNA was reverse transcribed into cDNAs in a final reaction volume of 20 μl using the Moloney Murine Leukemia Virus Reverse Transcriptase (M−MLV RT; Promega, USA). Finally, 1 μl of cDNA was amplified by the Corbett thermal cycler (Corbett Research, Australia) in the presence of forward and reverse primers (500 nM) and 2X Power SYBR Green Master Mix (Invitrogen) under the following conditions: pre-denaturation at 95 °C for 5 min, 35 cycles of denaturation at 94 °C for 30 s, annealing at 57 °C for 20 s, elongation at 72 °C for 30 s, and final elongation at 72 °C for 5 min. All assays were run in triplicate with the same samples, and the target gene expression was normalized with glyceraldehyde 3-phosphate dehydrogenase (GAPDH) as an internal control. The relative changes in gene expression were calculated using the $2^{-\Delta\Delta Ct}$ method. Table 1 shows the primer sequences that were obtained from a previous study [34].

2.10. Statistical analysis

To analyze the data, SPSS Statistics 20.0 was employed (SPSS Inc., Chicago, Illinois, USA). The Shapiro-Wilk test was applied to determine the data's normality. A one-way analysis of variance (ANOVA) was used to identify the statistically significant differences between the groups. To compare the groups, a Tukey-post hoc analysis was used. $P < 0.05$ were considered statistically significant, and all data were presented as standard deviations (SD).

Table 1
Specific primers sequences, at a final concentration of 500 nM, for real-time PCR.

Primer	Sequence
NGF	F: 5′-ACA CTC TGA TCA CTG CGT TTT TG-3′ R: 5′-CCT TCT GGG ACA TTG CTA TCT GT-3′
VEGF	F 5′-GAT CAT GCG GAT CAA ACC TC-3′ R 5′-AAT GCT TTC TCC GCT CTG AA-3′
BDNF	F 5′-CCATAAGGACGCGGACTTGTAC-3′ R 5′-AGACATGTTTGCGGCATCCAGG-3′
GAPDH	F 5′- CATCACTGCCACCCAGAAGACTG −3′ R 5′- ATGCCAGTGAGCTTCCCGTTCAG −3′

3. Results

This study aimed to assess the neuroprotective effects of IL-33 in a mouse sciatic nerve crush model. Due to a lack of significant differences with the sham group and for simplicity, the data from the healthy control group were not shown. All animals survived the experiment with no symptoms of neuroma or inflammation.

3.1. Motor function recovery

Following sciatic nerve injury, locomotor function is assessed via walking track analysis and rated by the SFI value. The locomotor assay was conducted every two weeks up to the 8th week post-operatively. As shown in Fig. 1, all groups had an appropriate motor function and normal SFI scores with no significant difference before surgery. Two weeks after surgery, however, all mice with sciatic nerve injuries had complete leg paralysis, and their mean SFI values tended toward −100. Over the next few weeks, all groups showed tendencies to improve in motor functions and SFI values. However, motor function recovery and the mean SFI value were significantly improved in mice given 50 μg/kg IL-33 compared to other nerve deficit groups at the 2nd, 4th, and 6th weeks after injury (Fig. 1; $P < 0.05$). At the end of the experiment, mice given 50 μg/kg IL-33 exhibited no significant difference in mean SFI from animals given 25 μg/kg IL-33 or sham groups. However, they were still significantly superior to the control and mice treated with 10 μg/kg IL-33 (Fig. 1; $P < 0.05$). Similarly, the mean SFI for mice given 25 μg/kg of IL-33 was significantly higher than for mice given 10 μg/kg of IL-33 and control groups at the 4th and 6th weeks postoperatively ($P < 0.01$). However, there was no statistically significant difference in terms of mean SFI values between the mice given 10 μg/kg of IL-33 and the controls. Further, sham surgery did not affect the SFI score. These findings revealed that animals treated with a higher dose of IL-33 had improved motor axon regeneration.

3.2. Sensory recovery evaluation

The recovery of sensory function was assessed via withdrawal responses to thermal stimulation. Fig. 2 depicts the hot plate test results for the six groups pre-operatively and then 2, 4, 6, and 8 weeks after surgery. In all animals with sciatic nerve injury, the thermal PWRL increased rapidly, reaching the cut-off value of 10 s two weeks after surgery, indicating severe sensory impairment. However, in the following weeks, sensory function and the PWRL improved progressively at various rates in all experimental groups. This finding confirms hind paw skin reinnervation (Fig. 2). According to the findings, IL-33 treatment at all three doses significantly reduced PWRL compared to the control group ($P < 0.01$). Among the IL-33-treated groups, PWRL for mice given 50 μg/kg of IL-33 was significantly lower than the others at the 4th and 6th weeks postoperatively, indicating a reduction in thermal pain threshold for this group ($P < 0.05$). In the eighth week, there was no statistically significant difference in mean PWRL between the 50 μg/kg and 25 μg/kg groups, although the 50 μg/kg dose of IL-33 was still superior to the 10 μg/kg dose, and the control group. In the same way, PWRL for mice given 25 μg/kg of IL-33 was significantly decreased compared to mice given 10 μg/kg of IL-33 at the 2nd, 4th, and 6th weeks postoperatively ($P < 0.01$). However, no significant difference was observed between the two groups in the 8th week. Additionally, the reduction of thermal pain threshold and subsequent PWRL in the 10 μg/kg IL-33 group was significantly greater than that in the control group in the 4th-week post-surgery (Fig, 2; $P < 0.05$). The PWRL was unaffected by sham surgery. These results demonstrated that IL-33 treatment could significantly reduce the thermal pain threshold in mice with sciatic nerve injuries.

3.3. Assessment of neural recovery with electrophysiological results

An electrophysiological measurement was performed in the fourth and eighth weeks after surgery to qualify the CMAP amplitudes and onset latency of CMAPs in the hind limbs. At the end of the fourth week, mice treated with 50 μg/kg of IL-33 had significantly higher mean CMAP amplitude (Fig. 3A; $P < 0.01$) and lower onset latency of CMAPs (Fig. 3B; $P < 0.01$) than other groups with nerve injury. Furthermore, in both measures, mice given 25 μg/kg IL-33 outperformed mice given 10 μg/kg IL-33 and controls ($P < 0.01$). However, no significant difference was observed between the 10 μg/kg IL-33 and control groups in the fourth week postoperatively. On the other hand, the mean CMAP amplitude in the experimental groups achieved a normal range at the end of the experiment with no significant difference (Fig. 3B). One of the causes of

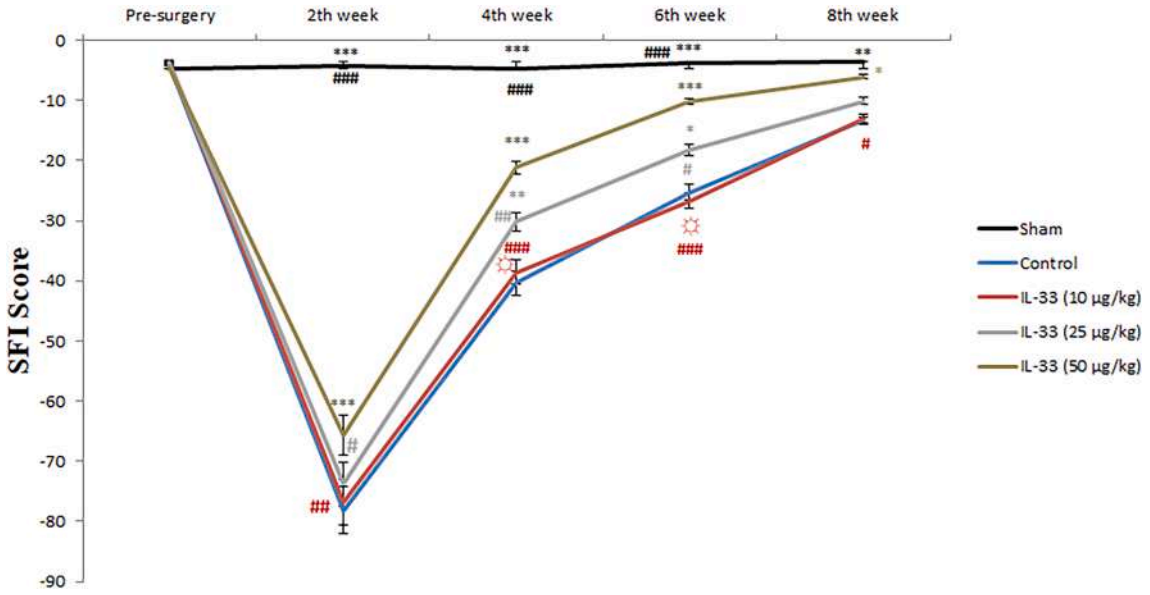

Fig. 1. Effect of IL-33 on sciatic function index (SFI). The SFI was assessed before surgery and every two weeks for the next eight weeks to determine motor function recovery. One-way analysis of variance and Tukey's post-hoc tests were used to analyze data. Data are presented as mean ± standard deviation (SD) (n = 10). * $P < 0.05$, ** $P < 0.01$, and ***$P < 0.001$ vs. control group; # $P < 0.05$, ## $P < 0.01$, and ### $P < 0.001$ vs. IL-33 (50 μg/kg) group; and ☼ $P < 0.05$ for comparison between IL and 33 (10 μg/kg) and IL-33 (25 μg/kg) groups.

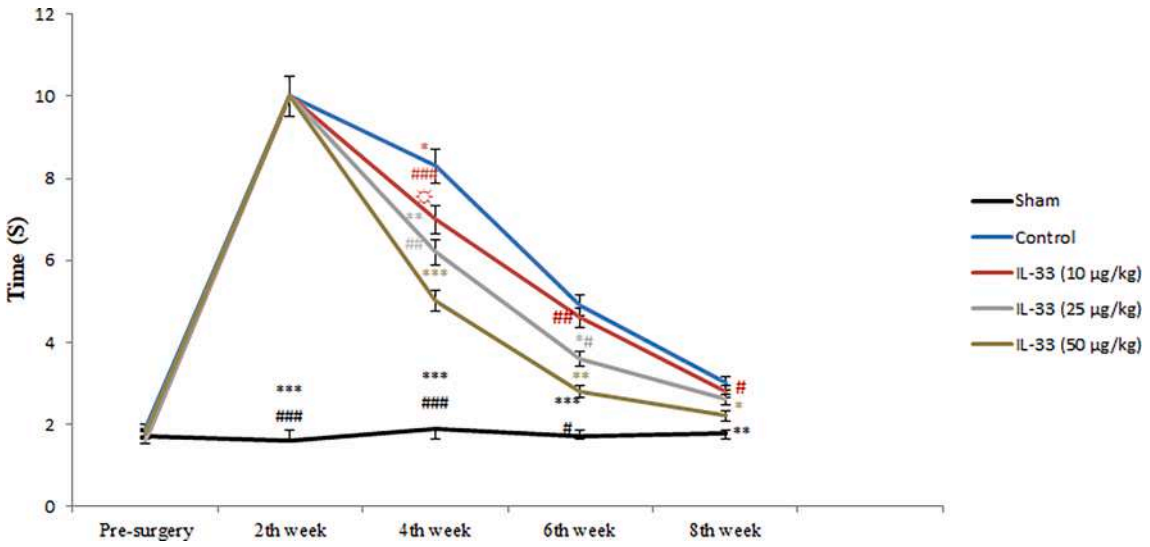

Fig. 2. Effect of IL-33 on the thermal paw withdrawal reflex latency (PWRL) before surgery and every two weeks for the next eight weeks. One-way analysis of variance and Tukey's post-hoc tests were used to analyze data. Data were expressed as mean ± standard deviation (SD) (n = 10). * P < 0.05, ** P < 0.01, and ***P < 0.001 vs. control group; # P < 0.05, ## P < 0.01, and ### P < 0.001 vs. IL-33 (50 µg/kg) group; and ☼ P< 0.05 for comparison between IL and 33 (10 µg/kg) and IL-33 (25 µg/kg) groups.

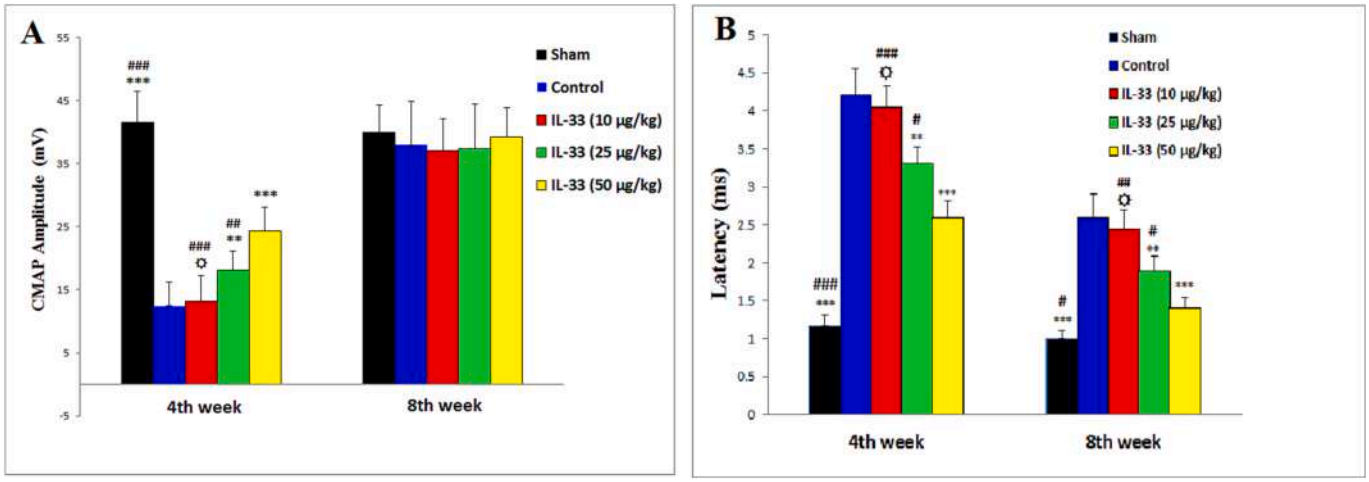

Fig. 3. Electrophysiological analysis. The compound muscle action potential (CMAP) and onset latency of CMAP were assessed in the 4th and 8th weeks post-operatively. (A) Results of CMAP amplitude after proximal stimulation of operated sciatic nerves in mice. (B) The onset latency of CMAP of the nerve after injury. One-way analysis of variance and Tukey's post-hoc tests were used to analyze data. Data were expressed as mean ± standard deviation (SD) (n = 10). ** P < 0.01 and ***P < 0.001 vs. control group; # P < 0.05, ## P < 0.01, and ### P < 0.001 vs. IL-33 (50 µg/kg) group; and ☼ P < 0.05 for comparison between IL and 33 (10 µg/kg) and IL-33 (25 µg/kg) groups.

the amplitude reaching normal levels could be the enlargement of the motor units in the regenerated motor axons. However, the mean CMAP latency was considerably reduced in mice treated with 50 µg/kg IL-33 compared to other nerve injury groups (P < 0.05). Similarly, mice given 25 µg/kg IL-33 outperformed those given 10 µg/kg IL-33. Conversely, no statistically significant difference in CMAP latency was observed between the 10 µg/kg IL-33 and control groups. These results revealed that animals treated with higher dosages of IL-33 had significantly increased excitability and conductivity, indicating effective axonal regeneration and gastrocnemius muscle reinnervation.

3.4. Evaluation of histomorphometric results

Fig. 4 shows toluidine blue staining of regenerated axons in the distal segment of injured sciatic nerves. Accordingly, Table 2 provides a morphometric analysis of the sciatic nerves. The results showed that mice treated with 50 µg/kg IL-33 had significantly higher myelinated fiber count, fiber diameter, axon diameter, and myelin thickness when compared with two other IL-33-treated groups and controls (P < 0.05). Similarly, in the above parameters, mice given 25 µg/kg IL-33 outperformed mice given 10 µg/kg IL-33 (P < 0.05). Further, no significant difference was observed between the 10 µg/kg IL-33 and control groups. Also, the mice given 50 µg/kg of IL-33 had a better g-ratio than mice given two other dosages of IL-33. The g-ratio is defined as axonal diameter/fiber diameter in myelinated axons and is an appropriate index of nerve fiber maturation and conduction efficiency. The previous study suggests that the optimal g-ratio is between 0.6 and 0.75.

3.5. Polarization of Macrophages in sciatic nerve

To evaluate the effects of IL-33 on macrophage polarization, the number of CD68+ (total macrophages), CD68 + CCR7+ (M1

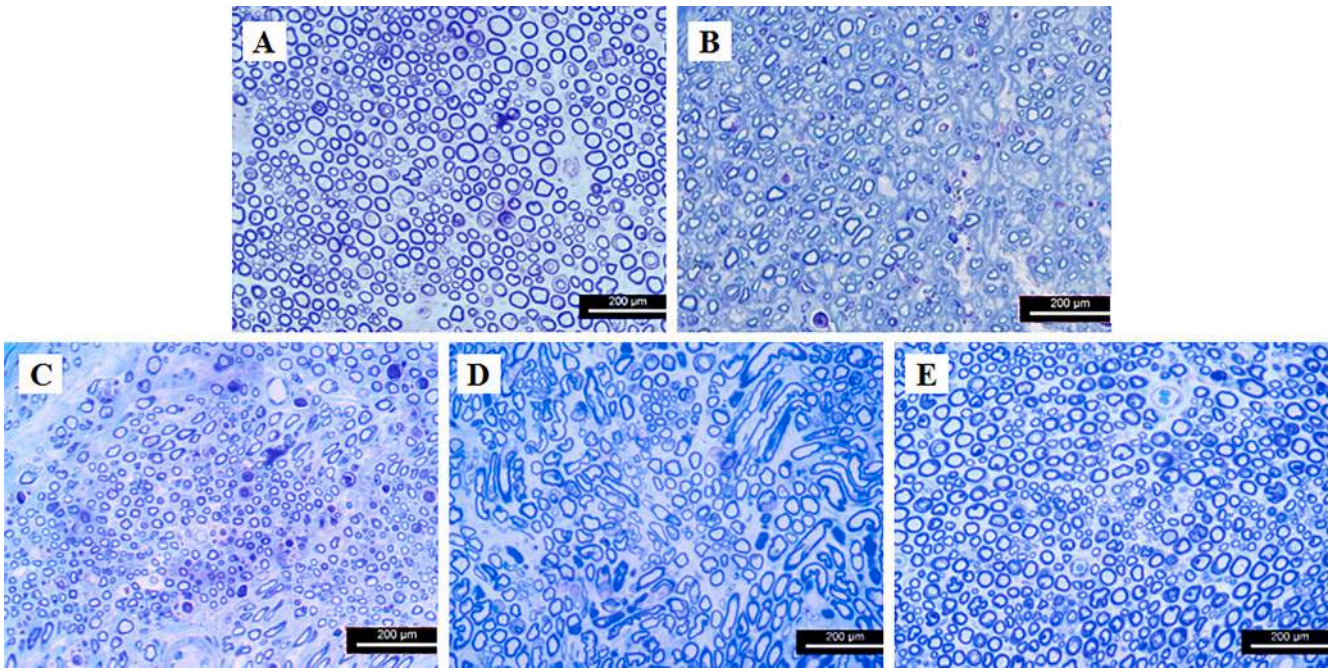

Fig. 4. Toluidine blue staining of regenerated nerves at the end of the experiment. (A) Sham group, (B) control group, (C) IL-33 (10 µg/kg), (D) IL-33 (25 µg/kg), and (E) IL-33 (50 µg/kg).

Table 2
Histomorphometric evaluation of myelinated axons in regenerated sciatic nerve cross-sections at the end of 8th week after surgery. Values are shown as mean ± SD (n = 10). * P < 0.05, ** P < 0.01, and *** P < 0.001 for comparison with control group; # P < 0.05, ## P < 0.01, and ### P < 0.001 for comparison with IL-33 (50 µg/kg) group; and ☼ P < 0.05 and ☼☼ P < 0.01 and ### P < 0.001 for comparison with IL-33 (50 µg/kg) group.

	Myelinated Fiber Count	Myelinated Fiber Diameter (µm)	Axon Diameter (µm)	Myelin Sheath Thickness (µm)	g-Ratio
Sham	4077 ± 280 ** ###	5.19 ± 0.86 *** #	3.15 ± 0.56 **	1.02 ± 0.21 *** #	0.61
Control	4592 ± 627	3.07 ± 0.72	2.39 ± 0.42	0.34 ± 0.11	0.78
IL-33 (10 µg/kg)	4533 ± 905 ☼ ##	3.11 ± 0.96 ☼☼ ###	2.33 ± 0.77 ☼ ##	0.39 ± 0.18 ☼☼ ###	0.75
IL-33 (25 µg/kg)	4839 ± 1003 * ##	3.84 ± 1.19 ** ##	2.62 ± 1.02 * #	0.61 ± 0.21 ** ##	0.68
IL-33 (50 µg/kg)	5418 ± 1584 **	4.70 ± 0.77 ***	2.96 ± 0.16 **	0.87 ± 0.18 ***	0.63

macrophages), and CD68 + CD206+ (M2 macrophages) cells at the injury site was measured using the immunostaining method (Fig. 5A). Although CD68 + CCR7 + and CD68 + CD206 + cells were found in all groups, mice administered 50 µg/kg of IL-33 had significantly fewer CD68 + CCR7 + cells (Fig. 5D; P < 0.001) and significantly more CD68 + CD206 + cells (Fig. 5E; P < 0.001) than the other groups. Furthermore, the highest total number of macrophages at the injury site was observed in the 50 µg/kg IL-33 group (Fig. 5; P < 0.01). Similarly, in mice given 25 µg/kg of IL-33, the total macrophage number (Fig. 5B) and percentage of CD68 + CD206 + cells were higher than in those given 10 µg/kg of IL-33 and controls (Fig. 5; P < 0.01). Nevertheless, no significant difference was observed between animals treated with 10 µg/kg IL-33 and the control group. As a result, IL-33 at doses of 50 µg/kg and 25 µg/kg could significantly increase the macrophage numbers and polarize them toward the M2 phenotype at the injured nerve.

3.6. Analysis of ELISA assay results

The ELISA test was used to determine the concentrations of IL-6 and IL-1β, which are responsible for the pro-inflammatory M1 response, and IL-4 and IL-10, which are responsible for the anti-inflammatory M2 response, at the injured nerves. As shown in Fig. 6, the concentration of IL-1β and IL-6 was significantly lower in mice treated with 50 µg/kg of IL-33 compared to those treated with 25 and 10 µg/kg of IL-33 (P < 0.05). In contrast, when mice were given 50 µg/kg of IL-33, the concentrations of anti-inflammatory cytokines (IL-4 and IL-10) were significantly elevated (P < 0.05). Similarly, once compared to a dose of 10 µg/kg, administration of IL-33 at a dose of 25 µg/kg significantly reduced IL-1β and IL-6 concentrations while increasing IL-4 and IL-10 concentrations (Fig. 6; P < 0.05). Nevertheless, there was no significant difference between mice given a 10 µg/kg dose of IL-33 and controls. These results showed that IL-33 at 50 and 25 µg/kg doses produced an anti-inflammatory effect and could promote a type 2 immune response in mice with sciatic nerve injury.

3.7. Quantitative real-time PCR analyses of the regenerated nerve

Sciatic nerves were subjected to real-time PCR two weeks after injury to assess the mRNA expression levels of VEGF, NGF, and BDNF. Fig. 7 shows that mice treated with 50 µg/kg of IL-33 had significantly higher levels of VEGF, NGF, and BDNF compared to mice treated with 25 µg/kg of IL-33 ($P < 0.05$). On the other hand, VEGF, NGF, and BDNF expression were significantly higher with IL-33 at 25 µg/kg compared to 10 µg/kg ($P < 0.05$). No significant difference was observed between the 10 µg/kg IL-33-treated group and the control group.

4. Discussion

Annually, more than 5 million new cases of PNI are diagnosed

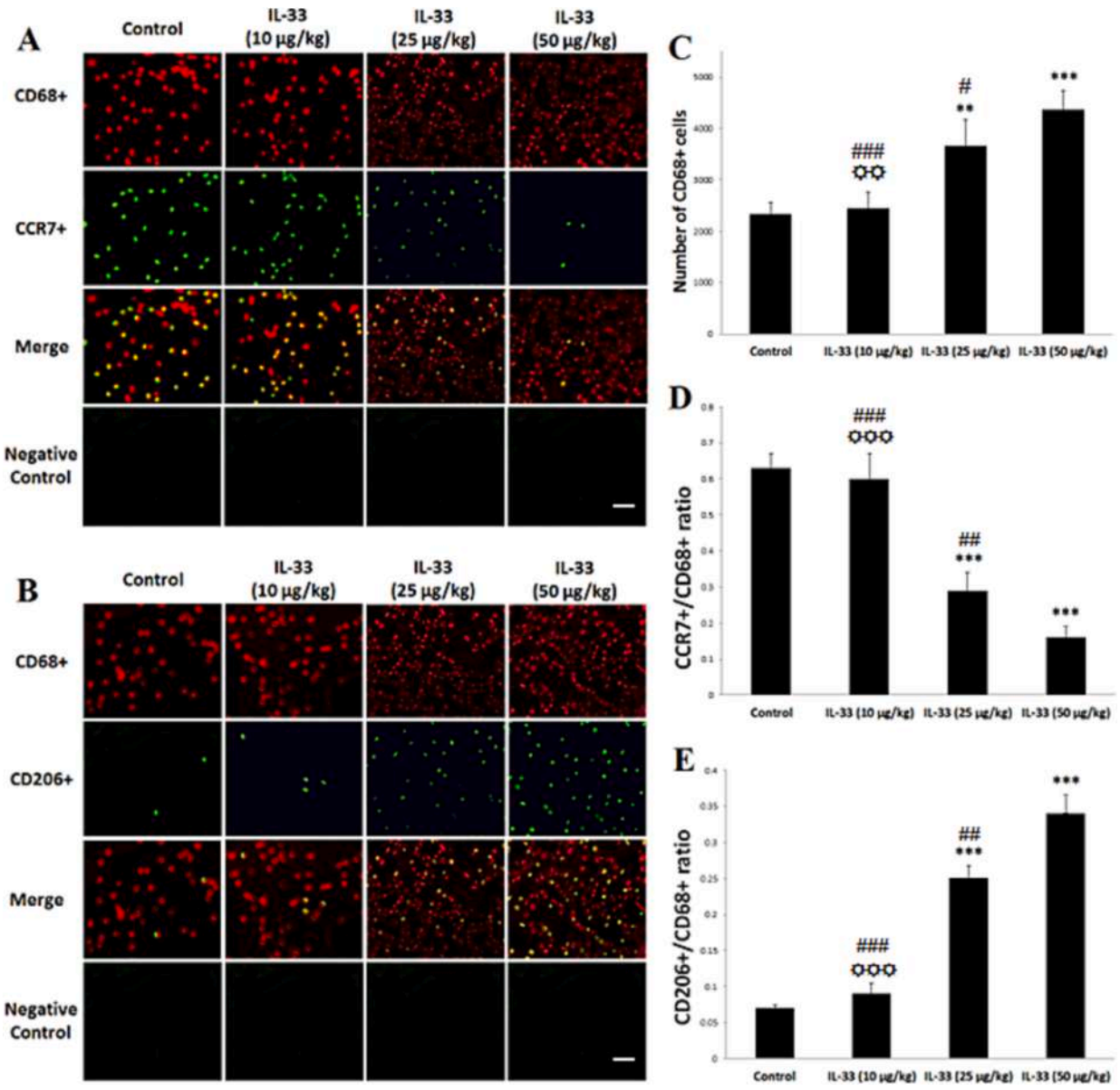

Fig. 5. Macrophages characterization in injured sciatic nerves. (A) Representation of double immunofluorescent staining of [(CD68+ (red)/CCR7+ (green)] macrophages (M1). Additionally, negative control staining without primary antibody (Secondary antibody alone) shows negative results with no detectable macrophage markers labeling. (B) Immunofluorescent staining of [(CD68+ (red)/CD206+ (green)] macrophages (M2). Negative control staining (Secondary antibody alone) shows negative results. Scale bar (50 µm). (C) Quantitative assessment of the total macrophage count. (D) The CCR7+/CD68 + ratio. (E) The CD206+/CD68 + ratio. One-way analysis of variance and Tukey's post-hoc tests were used to analyze data. Data were expressed as mean ± standard deviation (SD) (n = 4). ** $P < 0.01$ and ***$P < 0.001$ vs. control group; ##$P < 0.01$ and ### $P < 0.001$ vs. IL-33 (50 µg/kg) group; and ☼☼☼ $P < 0.001$ for comparison between IL and 33 (10 µg/kg) and IL-33 (25 µg/kg) groups.

worldwide, which results in sensorimotor dysfunction and reduced life quality [35,36]. Despite the innate regenerative capacity of peripheral nerves, regeneration after a severe injury is insufficient, and sensorimotor recovery is incomplete [1,37]. As a result, the development of alternative approaches to improving regeneration and sensorimotor recovery is essential. The current investigation examined the effects of IL-33 treatment in a sciatic nerve crush model in male C57BL/6 mice. IL-33 is a member of the IL-1 superfamily that is upregulated following pro-inflammatory conditions. This cytokine can be released from living cells or as an alarmin from necrotic cells following tissue injuries to warn the immune system. In immune cells such as T cells and macrophages, IL-33 mediates a Th2-like immune response by binding to the ST2 and IL-1RAP receptors. Its receptors are also expressed at relatively high levels in neural cells [38]. Following CNS injury, IL-33 via the Th2 cytokines polarizes macrophages toward the pro-healing M2 phenotype, which exerts anti-inflammatory activities, scavenges debris, and promotes angiogenesis and tissue repair [25]. Moreover, macrophages respond to peripheral nerve injury by facilitating the sprouting of axons into the distal segment of the injured nerves. Following nerve injury, hematogenous macrophages arrive at the lesion site within 24–48 h and reach their peak within 14–21 days [39]. This time frame is comparable to the debris removal period during Wallerian degeneration, which typically begins 3–4 days after a nerve injury and lasts 12–14 days [9]. The activity of the M1 macrophage phenotype during the first few days after nerve injury promotes Wallerian degradation via activation of SCs, debris phagocytosis, and immune cell recruitment to the injury site. However, chronic M1 macrophage activity at the lesion site leads to increased inflammatory cytokines, oxidative stress, neural death, and

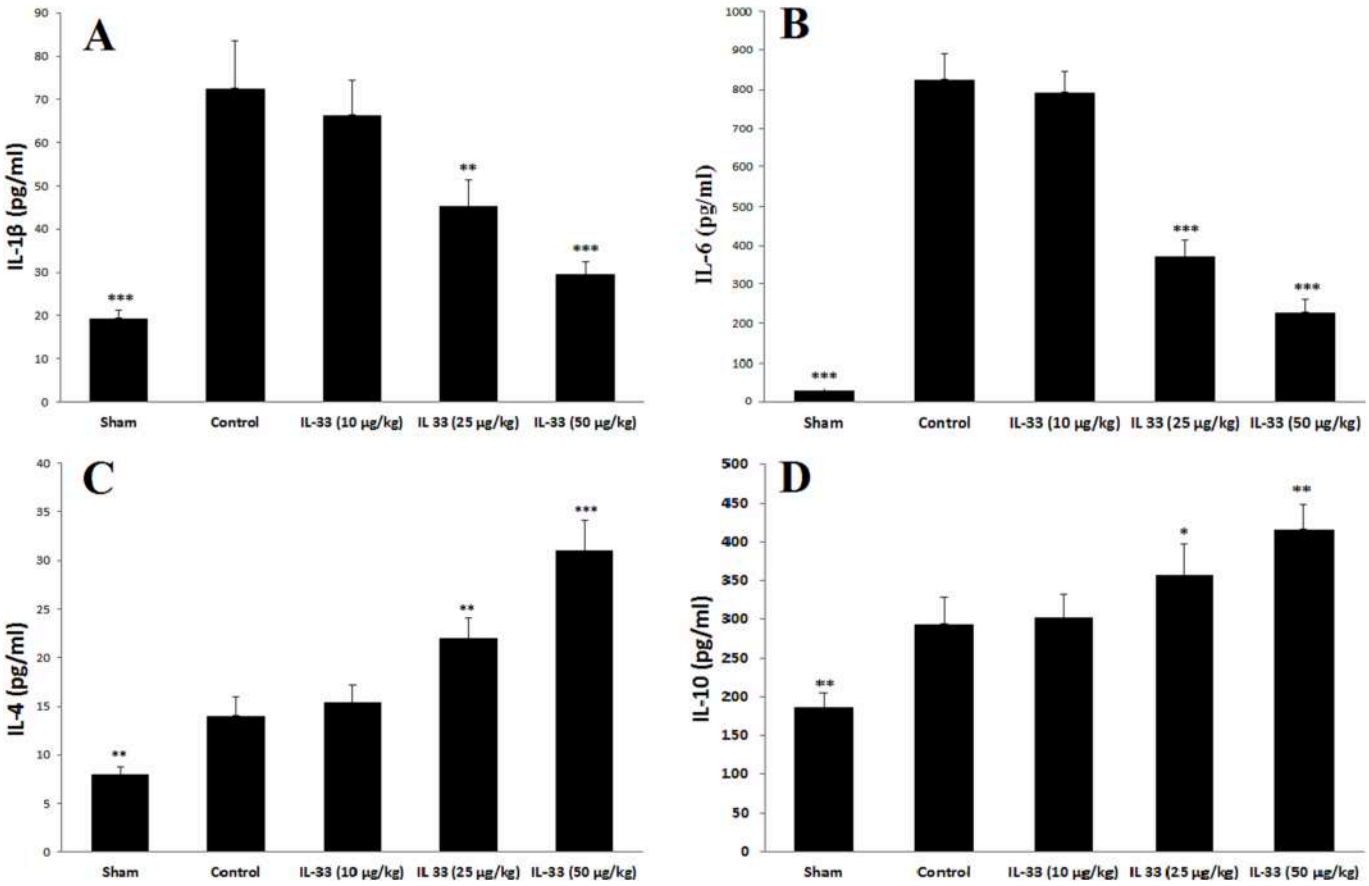

Fig. 6. Effects of IL-33 on the cytokine secretion in mouse sciatic nerve two weeks after sciatic nerve injury determined by ELISA. (A) IL-1β, (B) IL-6, (C) IL-4, and (D) IL-10. One-way analysis of variance and Tukey's post-hoc tests were used to analyze data. Data were expressed as mean ± standard deviation (SD) (n = 4). ** P < 0.01 and ***P < 0.001 vs. control group; # P < 0.05, ## P < 0.01, and ### P < 0.001 vs. IL-33 (50 µg/kg) group; and ☼ P < 0.05 for comparison between IL and 33 (10 µg/kg) and IL-33 (25 µg/kg) groups.

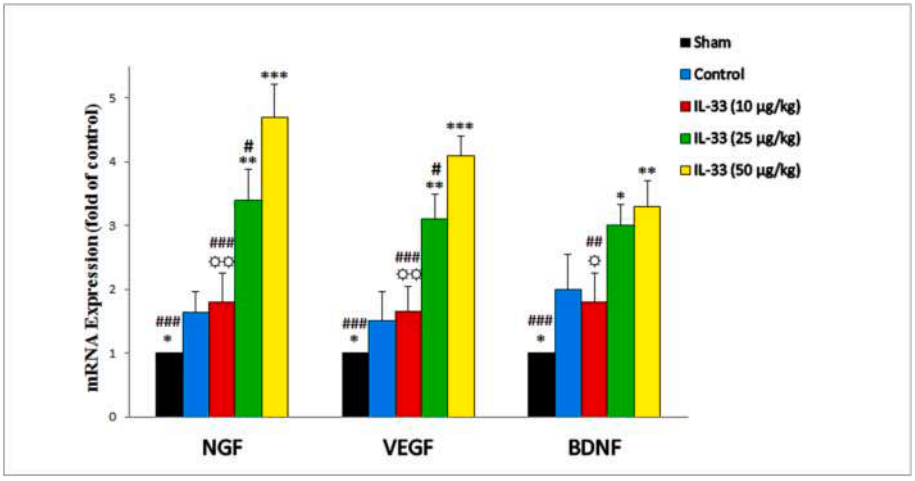

Fig. 7. The effects of IL-33 on NGF, VEGF, and BDNF mRNA expression in the sciatic nerves. The mRNA level in healthy mice has been attributed a value of 1 and the vertical axis numbers indicate relative changes from this baseline for each group. One-way analysis of variance and Tukey's post-hoc tests were used to analyze data. Data were expressed as mean ± standard deviation (SD) (n = 4). ** P < 0.01 and ***P < 0.001 vs. control group; # P < 0.05, ## P < 0.01, and ### P < 0.001 vs. IL-33 (50 µg/kg) group; and ☼ P < 0.05 for comparison between IL and 33 (10 µg/kg) and IL-33 (25 µg/kg) groups.

impaired nerve regeneration [1]. Therefore, macrophages must switch from the inflammatory M1 phenotype to the anti-inflammatory M2 phenotype after clearing the debris. Transitioning macrophages toward the pro-healing M2 phenotype is critical for reducing inflammation, promoting axonal regeneration, and inducing revascularization. M2 macrophages promote nerve regeneration by stimulating extracellular matrix remodeling and secreting a variety of substances, such as proteases and growth-promoting cytokines. The phenotype changes mainly occur around the 2nd-week post-injury, following Wallerian degeneration. As a result, modulating the macrophage phenotype toward the pro-healing M2 phenotype may be an effective therapeutic strategy for promoting nerve regeneration [40]. The macrophage polarization toward the pro-healing M2 phenotype can be examined in the second-week post-injury when debris has been cleared and axonal sprouts are growing in the distal part of the nerve.

Previous research has also emphasized the importance of the

macrophage phenotype as a therapeutic target in neural regeneration. In this regard, *Mokarram* and his colleagues conducted a study in the rat model to demonstrate the effect of macrophage phenotype on nerve regeneration via local delivery of interferon-gamma (IFN-γ) or IL-4 within a polymeric conduit. Their findings reveal that the ratio of M2 macrophages (CD206 +) to M1 macrophages (CCR7 +) is associated with the outcome of regeneration. Also, the polarization of macrophages toward the M2 phenotype in the injured nerve's distal segment could regulate SC activity and increase the number of sprouting axons. They concluded that the phenotype of macrophages at the injury site is more important than the number of macrophages for regenerative outcomes [16]. Moreover, some evidence suggests macrophages can regulate SC maturation and remyelination function following PNI. It is revealed that the elimination of macrophages from nerves elevated immature SC counts, decreased remyelination, and reduced nerve conduction velocity [14]. *In-vitro* studies demonstrated that macrophages, via expression of IL-6 and growth arrest-specific 6 (Gas6), can regulate SC maturation and remyelination function [41]. On the other hand, although IL-33 through macrophages could indirectly affect SCs, there is insufficient information about the direct interaction between IL and 33 and SCs during nerve regeneration. In another study on macrophage phenotypes, *Kuo et al.* (2011) found that polarizing macrophages toward the M2 phenotype under acid fibroblast growth factor (aFGF) treatment could improve neurotrophic factor secretion and axonal regeneration in rats with spinal cord injury [42]. Furthermore, studies have shown that activating the IL-33/ST2 signaling pathway after an ischemic stroke reduces neuronal damage by shifting microglial and macrophage polarization toward the M2 phenotype and, as a result, increasing the secretion of type 2-response-associated cytokines [22,43]. As a result, we hypothesized that seven days of recombinant IL-33 therapy improves functional recovery by shifting the type 1 immune response toward the type 2 immune response in mice with sciatic nerve impairment. Furthermore, we only used low concentrations of IL-33 in this study because some research has shown that high concentrations (50 μg/kg) of IL-33 induce a pro-inflammatory type 1 immune response, whereas lower concentrations (10 μg/kg) induce an anti-inflammatory type 2 immune response [44]. We also measured neurotrophic factor expression, cytokine secretion, and macrophage polarization two weeks following surgery, so some research has indicated that the peak of macrophage infiltration, cytokine secretion, and neurotrophic factor expression occurs 7–14 days after nerve injury [45,46]. In brief, our findings suggest that seven days of IL-33 treatment immediately following a sciatic nerve injury could significantly accelerate the restoration of sensory and motor functions. Altogether, our findings confirmed IL-33 therapy's efficacy in promoting axonal regeneration and target organ reinnervation in mice with sciatic nerve deficits. IL-33 modulates various immune cells, including T cells and macrophages, mediating the Th2-like immune response and tissue repair. IL-33 has been shown to polarize macrophages toward the pro-healing M2 phenotype by increasing the release of Th2 cytokines such as IL-4, IL-5, and IL-13 [47,48]. ELISA and immunohistochemical assays, on the other hand, revealed that IL-33 treatment at both doses could significantly polarize macrophages toward the pro-healing M2 phenotype (CD68 + CD206 +) and increase the total number of macrophages in injured nerves. In addition, mice treated with 50 and 25 μg/kg of IL-33 showed a significant reduction in pro-inflammatory cytokine (IL-1β and IL-6) levels and an increase in anti-inflammatory cytokine (IL-4 and IL-10) secretion at the injured site. Liu and his colleagues showed that in the peripheral nerves, macrophages are distributed in the epineurium and endoneurium. These cells respond to nerve injury by facilitating the sprouting of axons into the distal segment of the degenerated nerve via the Büngner bands [18]. Further, macrophages can polarize into the M1 or M2 phenotype based on their microenvironment. Generally, M2 macrophages are anti-inflammatory and provide a supportive microenvironment for axonal regeneration [40]. The real-time PCR also demonstrated that mice treated with IL-33 had significantly higher levels of NGF, VEGF, and BDNF expression. Evidence suggests that NGF plays a significant role in sensory nerve regeneration and sensory function recovery by stimulating sensory neuron sprouting and survival. Similarly, BDNF can improve neuron survival, neurite outgrowth, and neuroplasticity following nerve injury. It also decreases proinflammatory cytokine release from macrophages while not affecting cytokine mRNA expression [49]. The expression of VEGF is also essential for angiogenesis. Some evidence suggests that IL-33/ST2 signaling is involved in hypersensitization behaviors. For example, *Wang et al.* (2022) demonstrated that the IL-33/ST2 signaling pathway induces sensory nerve hyperexcitability via inhibiting A-type K + channels. This finding may explain why a low dose of IL-33 improves sensory recovery in mice with sciatic nerve injuries. On the other hand, the collateral reinnervation of polymodal unmyelinated C axons, which are primarily responsible for thermal pain, may account for the significant drop in the thermal pain threshold in the 10 μg/kg IL-33 group compared to controls [50]. However, these fibers were too thin to count using light microscopy. Further, some evidence suggests that cytokines produced by invasive macrophages may develop thermal hyperalgesia following nerve injury [51,52]. Although the effect of IL-33 in traumatic PNI is not apparent, various studies have investigated the neuroprotective effects of IL-33 therapy against CNS disorders. Evidence suggests that local secretion of IL-33 is increased immediately after CNS injury and triggers immune responses at the lesion site [53]. Also, in another study, Zhang and his colleagues showed that injection of intravenous immunoglobulin and sialylated intravenous immunoglobulin in C57BL/6 mice upregulates the gene expression of IL-33, which itself can protect from antibody-mediated nerve injury through the SIGN-R1-Th2 pathway. Also, elements of this pathway, including IL-33 can provide novel therapeutics for inflammatory neuropathies [54].

In contrast to M1 macrophages, which are associated with secondary injury progression following spinal cord injury (SCI), M2 macrophages are involved in oligodendrocyte differentiation, axon remyelination, and sensorimotor recovery. However, M2 macrophages disappear within one week after SCI, so any therapeutic intervention that increases the number of M2 macrophages may enhance the spinal cord's regenerative capacity. In this regard, *Pomeshchik et al.* (2015) found that recombinant IL-33 could promote the activation of anti-inflammatory M2 macrophages and microglia at the injury site in a contused mouse spinal cord model. Further, IL-33 reduces astrogliosis, diminishes tissue loss, suppresses demyelination, and improves sensorimotor recovery [25]. Furthermore, IL-33 therapy is effective in the treatment of neurovascular complications such as ischemic and hemorrhagic strokes. For example, Gao et al. (2017) reported the neuroprotective effects of IL-33 against intracerebral hemorrhage in mice. They discovered that IL-33 treatment reduced inflammation and inhibited apoptosis in damaged tissues [55]. *Yang et al.* (2017) found that the IL-33/ST2 signaling pathway could polarize macrophages toward an M2 phenotype and reduce neuronal death during brain ischemia [22]. In line with this finding, *Jiang et al.* (2018) discovered that enhancing the IL-33/ST2 signaling pathway could reduce ischemic stroke-induced brain damage in rat models of middle cerebral artery occlusion (MCAO), likely by promoting the polarization of microglia and macrophages toward M2 phenotypes [56]. In another study on intracerebral hemorrhage in rats, *Chen et al.* (2019) discovered that intracerebroventricular injection of IL-33 decreased neuronal death and white matter injury, therefore attenuating neurological consequences. IL-33 expression was also upregulated in microglia and astrocytes surrounding the hematoma. They explain that the neuroprotective effects of IL-33 are related to the polarization of microglia and macrophages toward the anti-inflammatory M2 phenotype [57].

Finally, our study discovered that the sensory-motor recovery period, as well as the number of regenerating axons in the distal nerve stumps, were significantly higher than in some previous mouse nerve crush studies. We argued that crush injury models lack a standardized method and can cause varying degrees of nerve damage, ranging from

Sunderland II to IV, depending on factors such as force, duration, and extent of nerve compression [26,58]. In the present study, we crushed the sciatic nerve at the sciatic notch using serrated right-angle forceps with a 2.5-mm tip width. The nerve was compressed twice in perpendicular directions, each time for 30 s. It seems that prolonged compression by serrated forceps in perpendicular directions results in a severe nerve crush injury, likely due to the disruption of the endoneurium and perineurium. In other words, although the continuity of the nerve is maintained, the endoneurium and epineurium may be interrupted. Therefore, our methodology differs from studies that used non-serrated forceps and shorter compression durations. Furthermore, when compared to studies that induced nerve crush around the sciatic nerve bifurcation, the proximity of the lesion site to the spinal cord may explain the prolonged sensory and motor recovery in our study. The regenerating axons in the nerve crush at the level of the sciatic notch take a longer route to innervate the target organs than downstream injuries. Moreover, the proximity of the lesion site to the spinal cord increases the sensory and motor neuron death rates. The high number of regenerating axons in injured nerves could also be explained by axon collateral sprouting triggered by endoneurium disruption. In addition, the increase in the number and density of regenerating axons and prolonged functional recovery can be observed in several studies conducted on mild crash models [59,60]. It is worth mentioning that axons with no functional synapses are eliminated after a few months, and fiber numbers return to normal. Taken together, we argue that the aforementioned factors may explain the prolonged sensory-motor recovery observed in our study.

5. Conclusions

This study demonstrates that recombinant IL-33 administration for seven days could significantly accelerate regeneration and improve sensorimotor recovery. According to our findings, IL-33 significantly polarized macrophages toward the M2 phenotype and attenuated the pro-inflammatory response in the injured nerve. The IL-33 treatment appears to be a promising approach to managing PNI and minimizing its consequences. More research is needed, however, to confirm these findings.

6. Limitations

1) In this research, the nerves didn't stain for the presence of other immune cell populations, and we propose to do it in future work because a more expansive approach may have revealed changes in other inflammatory cells.
2) Future studies will need to check other genes, like key markers of the SCs lineage (S100 and p75).

CRediT authorship contribution statement

Shukur Wasman Smail: Conceptualization, Investigation, Writing – review & editing. **Shang Ziyad Abdulqadir:** Data curation, Investigation. **Zhikal Omar Khudhur:** Data curation, Investigation. **Sonia Elia Ishaq:** Data curation. **Abdullah Faqiyazdin Ahmed:** Formal analysis, Writing – review & editing. **Mohammad B. Ghayour:** Conceptualization, Writing – review & editing. **Arash Abdolmaleki:** Conceptualization, Data curation, Formal analysis, Investigation, Writing – review & editing.

Declaration of Competing Interest

The authors declare that they have no known competing financial interests or personal relationships that could have appeared to influence the work reported in this paper.

Data availability

Data will be made available on request.

Acknowledgments

We thank the Research Council of Salahaddin University and the University of Mohaghegh Ardabili for their financial support of this project University of Mohaghegh ArdabiliGrant numbers: 2243Ir and Salahaddin University - Erbil Grant numbers: er2212.

References

[1] J. Scheib, A. Höke, Advances in peripheral nerve regeneration, Nat. Rev. Neurol. 9 (12) (2013) 668–676.
[2] S. Bolívar, X. Navarro, E. Udina, Schwann cell role in selectivity of nerve regeneration, Cells 9 (9) (2020) 2131.
[3] S. Ferdowsi, A. Abdolmaleki, A. Asadi, S. Zahri, Effect of Azithromycin on Sciatic Nerve Injury in the Wistar Rats, Neurochem. Res. (2022) 1–11.
[4] K. Zhang, M. Jiang, Y. Fang, The drama of Wallerian degeneration: the cast, crew, and script, Annu. Rev. Genet. 55 (2021) 93–113.
[5] H.F. Al-Saedi, H.A. Ghanimi, S.M. Khoshnazar, A. Abdolmaleki, Neuroprotective effects of celastrol on sciatic nerve transection model in male Wistar rats, Iran. J. Basic Med. Sci. 25 (10) (2022).
[6] M. Bautista, A. Krishnan, Self-renewal of peripheral nerve resident macrophage: does it represent a unique activation status? Neural Regen. Res. 17 (5) (2022) 999.
[7] J. Li, Y. Yao, Y. Wang, J. Xu, D. Zhao, M. Liu, S. Shi, Y. Lin, Modulation of the Crosstalk Between Schwann Cells and Macrophages for Nerve Regeneration: A Therapeutic Strategy Based on Multifunctional Tetrahedral Framework Nucleic Acids System, Adv. Mater. 2202513 (2022).
[8] P. Chen, X. Piao, P. Bonaldo, Role of macrophages in Wallerian degeneration and axonal regeneration after peripheral nerve injury, Acta Neuropathol. 130 (5) (2015) 605–618.
[9] S. Rotshenker, Wallerian degeneration: the innate-immune response to traumatic nerve injury, J. Neuroinflammation 8 (1) (2011) 1–14.
[10] R. Martini, S. Fischer, R. López-Vales, S. David, Interactions between Schwann cells and macrophages in injury and inherited demyelinating disease, Glia 56 (14) (2008) 1566–1577.
[11] A.D. Gaudet, P.G. Popovich, M.S. Ramer, Wallerian degeneration: gaining perspective on inflammatory events after peripheral nerve injury, J. Neuroinflammation 8 (1) (2011) 1–13.
[12] C.-Y. Lu, K.B. Santosa, A. Jablonka-Shariff, B. Vannucci, A. Fuchs, I. Turnbull, D. Pan, M.D. Wood, A.K. Snyder-Warwick, Macrophage-derived vascular endothelial growth factor-A is integral to neuromuscular junction reinnervation after nerve injury, J. Neurosci. 40 (50) (2020) 9602–9616.
[13] R.E. Zigmond, F.D. Echevarria, Macrophage biology in the peripheral nervous system after injury, Prog. Neurobiol. 173 (2019) 102–121.
[14] J.A. Stratton, A. Holmes, N.L. Rosin, S. Sinha, M. Vohra, N.E. Burma, T. Trang, R. Midha, J. Biernaskie, Macrophages regulate Schwann cell maturation after nerve injury, Cell reports 24(10) (2018) 2561-2572. e6.
[15] P.K. Govindappa, J.C. Elfar, Erythropoietin promotes M2 macrophage phagocytosis of Schwann cells in peripheral nerve injury, Cell Death Dis. 13 (3) (2022) 1–12.
[16] N. Mokarram, A. Merchant, V. Mukhatyar, G. Patel, R.V. Bellamkonda, Effect of modulating macrophage phenotype on peripheral nerve repair, Biomaterials 33 (34) (2012) 8793–8801.
[17] Z. Julier, A.J. Park, P.S. Briquez, M.M. Martino, Promoting tissue regeneration by modulating the immune system, Acta Biomater. 53 (2017) 13–28.
[18] P. Liu, J. Peng, G.-H. Han, X. Ding, S. Wei, G. Gao, K. Huang, F. Chang, Y. Wang, Role of macrophages in peripheral nerve injury and repair, Neural Regen. Res. 14 (8) (2019) 1335.
[19] G. Haraldsen, J. Balogh, J. Pollheimer, J. Sponheim, A.M. Küchler, Interleukin-33–cytokine of dual function or novel alarmin? Trends Immunol. 30 (5) (2009) 227–233.
[20] Y. Sun, Y. Wen, L. Wang, L. Wen, W. You, S. Wei, L. Mao, H. Wang, Z. Chen, X. Yang, Therapeutic opportunities of interleukin-33 in the central nervous system, Front. Immunol. 12 (2021), 654626.
[21] X.-M. Yi, H. Lian, S. Li, Signaling and functions of interleukin-33 in immune regulation and diseases, Cell, Insight (2022), 100042.
[22] Y. Yang, H. Liu, H. Zhang, Q. Ye, J. Wang, B. Yang, L. Mao, W. Zhu, R.K. Leak, B. Xiao, ST2/IL-33-dependent microglial response limits acute ischemic brain injury, J. Neurosci. 37 (18) (2017) 4692–4704.
[23] M. Kurowska-Stolarska, B. Stolarski, P. Kewin, G. Murphy, C.J. Corrigan, S. Ying, N. Pitman, A. Mirchandani, B. Rana, N. van Rooijen, IL-33 amplifies the polarization of alternatively activated macrophages that contribute to airway inflammation, J. Immunol. 183 (10) (2009) 6469–6477.
[24] W. Xiao, S. Guo, L. Chen, Y. Luo, The role of Interleukin-33 in the modulation of splenic T-cell immune responses after experimental ischemic stroke, J. Neuroimmunol. 333 (2019), 576970.
[25] Y. Pomeshchik, I. Kidin, P. Korhonen, E. Savchenko, M. Jaronen, S. Lehtonen, S. Wojciechowski, K. Kanninen, J. Koistinaho, T. Malm, Interleukin-33 treatment reduces secondary injury and improves functional recovery after contusion spinal cord injury, Brain Behav. Immun. 44 (2015) 68–81.

[26] P.M. Bridge, D.J. Ball, S.E. Mackinnon, Y. Nakao, K. Brandt, D.A. Hunter, C. Hertl, Nerve crush injuries—a model for axonotmesis, Exp. Neurol. 127 (2) (1994) 284–290.
[27] J. Bain, S. Mackinnon, D. Hunter, Functional evaluation of complete sciatic, peroneal, and posterior tibial nerve lesions in the rat, Plast. Reconstr. Surg. 83 (1) (1989) 129–138.
[28] L. Sarikcioglu, B. Demirel, A. Utuk, Walking track analysis: an assessment method for functional recovery after sciatic nerve injury in the rat, Folia Morphol. 68 (1) (2009) 1–7.
[29] K. Hargreaves, R. Dubner, F. Brown, C. Flores, J. Joris, A new and sensitive method for measuring thermal nociception in cutaneous hyperalgesia, Pain 32 (1) (1988) 77–88.
[30] A. Rupp, U. Dornseifer, A. Fischer, W. Schmahl, K. Rodenacker, U. Jütting, P. Gais, E. Biemer, N. Papadopulos, K. Matiasek, Electrophysiologic assessment of sciatic nerve regeneration in the rat: surrounding limb muscles feature strongly in recordings from the gastrocnemius muscle, J. Neurosci. Methods 166 (2) (2007) 266–277.
[31] A. Schulz, C. Walther, H. Morrison, R. Bauer, In vivo electrophysiological measurements on mouse sciatic nerves, JoVE (Journal of Visualized Experiments) 86 (2014) e51181.
[32] F.D. Scipio, S. Raimondo, P. Tos, S. Geuna, A simple protocol for paraffin-embedded myelin sheath staining with osmium tetroxide for light microscope observation, Microsc. Res. Tech. 71 (7) (2008) 497–502.
[33] N. Mokarram, K. Dymanus, A. Srinivasan, J.G. Lyon, J. Tipton, J. Chu, A. W. English, R.V. Bellamkonda, Immunoengineering nerve repair, Proc. Natl. Acad. Sci. 114 (26) (2017) E5077–E5084.
[34] F. Marrocco, M. Delli Carpini, S. Garofalo, O. Giampaoli, E. De Felice, M.A. Di Castro, L. Maggi, F. Scavizzi, M. Raspa, F. Marini, Short-chain fatty acids promote the effect of environmental signals on the gut microbiome and metabolome in mice, Commun. Biol. 5 (1) (2022) 1–13.
[35] W.A. Lackington, A.J. Ryan, F.J. O'Brien, Advances in nerve guidance conduit-based therapeutics for peripheral nerve repair, ACS Biomater Sci. Eng. 3 (7) (2017) 1221–1235.
[36] H.F. Al-Saedi, Y. Panahi, H.A. Ghanimi, A. Abdolmaleki, A. Asadi, Enhancement of nerve regeneration with nimodipine treatment after sciatic nerve injury, Fundam. Clin. Pharmacol. (2022).
[37] M.-B. Ghayour, A. Abdolmaleki, M. Behnam-Rassouli, The effect of memantine on functional recovery of the sciatic nerve crush injury in rats, Turk Neurosurg 27 (4) (2017) 641–647.
[38] J. Schmitz, A. Owyang, E. Oldham, Y. Song, E. Murphy, T.K. McClanahan, G. Zurawski, M. Moshrefi, J. Qin, X. Li, IL-33, an interleukin-1-like cytokine that signals via the IL-1 receptor-related protein ST2 and induces T helper type 2-associated cytokines, Immunity 23 (5) (2005) 479–490.
[39] R. George, J.W. Griffin, Delayed macrophage responses and myelin clearance during Wallerian degeneration in the central nervous system: the dorsal radiculotomy model, Exp. Neurol. 129 (2) (1994) 225–236.
[40] C. Yunna, H. Mengru, W. Lei, C. Weidong, Macrophage M1/M2 polarization, Eur. J. Pharmacol. 877 (2020), 173090.
[41] X. Dong, S. Liu, Y. Yang, S. Gao, W. Li, J. Cao, Y. Wan, Z. Huang, G. Fan, Q. Chen, Aligned microfiber-induced macrophage polarization to guide schwann-cell-enabled peripheral nerve regeneration, Biomaterials 272 (2021), 120767.
[42] H.-S. Kuo, M.-J. Tsai, M.-C. Huang, C.-W. Chiu, C.-Y. Tsai, M.-J. Lee, W.-C. Huang, Y.-L. Lin, W.-C. Kuo, H. Cheng, Acid fibroblast growth factor and peripheral nerve grafts regulate Th2 cytokine expression, macrophage activation, polyamine synthesis, and neurotrophin expression in transected rat spinal cords, J. Neurosci. 31 (11) (2011) 4137–4147.
[43] Q. Luo, Y. Fan, L. Lin, J. Wei, Z. Li, Y. Li, S. Nakae, W. Lin, Q. Chen, Interleukin-33 protects ischemic brain injury by regulating specific microglial activities, Neuroscience 385 (2018) 75–89.
[44] X. Rao, F. Hua, L. Zhang, Y. Lin, P. Fang, S. Chen, J. Ying, X. Wang, Dual roles of interleukin-33 in cognitive function by regulating central nervous system inflammation, J. Transl. Med. 20 (1) (2022) 1–16.
[45] S. Jander, F. Lausberg, G. Stoll, Differential recruitment of CD8+ macrophages during Wallerian degeneration in the peripheral and central nervous system, Brain Pathol. 11 (1) (2001) 27–38.
[46] M.E. Vargas, J. Watanabe, S.J. Singh, W.H. Robinson, B.A. Barres, Endogenous antibodies promote rapid myelin clearance and effective axon regeneration after nerve injury, Proc. Natl. Acad. Sci. 107 (26) (2010) 11993–11998.
[47] C. Wang, C. Dong, S. Xiong, IL-33 enhances macrophage M2 polarization and protects mice from CVB3-induced viral myocarditis, J. Mol. Cell. Cardiol. 103 (2017) 22–30.
[48] R. He, H. Yin, B. Yuan, T. Liu, L. Luo, P. Huang, L. Dai, K. Zeng, IL-33 improves wound healing through enhanced M2 macrophage polarization in diabetic mice, Mol. Immunol. 90 (2017) 42–49.
[49] H.-C. Yu, H.-B. Huang, H.-Y. Huang Tseng, M.-C. Lu, Brain-Derived Neurotrophic Factor Suppressed Proinflammatory Cytokines Secretion and Enhanced MicroRNA (miR)-3168 Expression in Macrophages, Int. J. Mol. Sci. 23 (1) (2022) 570.
[50] S. Cobianchi, J. de Cruz, X. Navarro, Assessment of sensory thresholds and nociceptive fiber growth after sciatic nerve injury reveals the differential contribution of collateral reinnervation and nerve regeneration to neuropathic pain, Exp. Neurol. 255 (2014) 1–11.
[51] T. Liu, N. van Rooijen, D.J. Tracey, Depletion of macrophages reduces axonal degeneration and hyperalgesia following nerve injury, Pain 86 (1–2) (2000) 25–32.
[52] C. Sommer, M. Schäfers, Painful mononeuropathy in C57BL/Wld mice with delayed wallerian degeneration: differential effects of cytokine production and nerve regeneration on thermal and mechanical hypersensitivity, Brain Res. 784 (1–2) (1998) 154–162.
[53] S.P. Gadani, J.T. Walsh, I. Smirnov, J. Zheng, J. Kipnis, The glia-derived alarmin IL-33 orchestrates the immune response and promotes recovery following CNS injury, Neuron 85 (4) (2015) 703–709.
[54] G. Zhang, C.A. Massaad, T. Gao, L. Pillai, N. Bogdanova, S. Ghauri, K.A. Sheikh, Sialylated intravenous immunoglobulin suppress anti-ganglioside antibody mediated nerve injury, Exp. Neurol. 282 (2016) 49–55.
[55] Y. Gao, L. Ma, C.-L. Luo, T. Wang, M.-Y. Zhang, X. Shen, H.-H. Meng, M.-M. Ji, Z.-F. Wang, X.-P. Chen, IL-33 exerts neuroprotective effect in mice intracerebral hemorrhage model through suppressing inflammation/apoptotic/autophagic pathway, Mol. Neurobiol. 54 (5) (2017) 3879–3892.
[56] M. Jiang, X. Liu, D. Zhang, Y. Wang, X. Hu, F. Xu, M. Jin, F. Cao, L. Xu, Celastrol treatment protects against acute ischemic stroke-induced brain injury by promoting an IL-33/ST2 axis-mediated microglia/macrophage M2 polarization, J. Neuroinflammation 15 (1) (2018) 1–12.
[57] Z. Chen, N. Xu, X. Dai, C. Zhao, X. Wu, S. Shankar, H. Huang, Z. Wang, Interleukin-33 reduces neuronal damage and white matter injury via selective microglia M2 polarization after intracerebral hemorrhage in rats, Brain Res. Bull. 150 (2019) 127–135.
[58] M. Caillaud, L. Richard, J.-M. Vallat, A. Desmoulière, F. Billet, Peripheral nerve regeneration and intraneural revascularization, Neural Regen. Res. 14 (1) (2019) 24.
[59] A.S. Varejão, A.M. Cabrita, M.F. Meek, J. Bulas-Cruz, P. Melo-Pinto, S. Raimondo, S. Geuna, M.G. Giacobini-Robecchi, Functional and morphological assessment of a standardized rat sciatic nerve crush injury with a non-serrated clamp, J. Neurotrauma 21 (11) (2004) 1652–1670.
[60] A. Luís, S. Amado, S. Geuna, J. Rodrigues, M. Simões, J. Santos, F. Fregnan, S. Raimondo, A.P. Veloso, A. Ferreira, Long-term functional and morphological assessment of a standardized rat sciatic nerve crush injury with a non-serrated clamp, J. Neurosci. Methods 163 (1) (2007) 92–104.